

Spin waves at surfaces and interfaces in cubic Heisenberg systems

Bu Xing Xu*

Department of Physics and Astronomy, Louisiana State University, Baton Rouge, Louisiana 70803

Mark Mostoller and A. K. Rajagopal†

Solid State Division, Oak Ridge National Laboratory, Oak Ridge, Tennessee 37831

(Received 3 December 1984)

The effects of the underlying crystal structure and the surface or interface normal on spin waves at surfaces and interfaces are examined for cubic crystals described by the Heisenberg Hamiltonian. For surfaces, cleavage and the Goldstone rule by themselves generally favor the formation of surface states. Interface states occur in nearly every case studied in simple model bicrystals. With the same perturbations, there are pronounced differences in the results obtained for different faces of the same crystal, or in those for the same face of different crystals.

I. INTRODUCTION

For systems described by tight-binding-like Hamiltonians of finite range, the elementary excitations at ordered surfaces and interfaces can be found by Green's-function treatments that amount to mappings onto linear chains. This was perhaps first shown in a classic paper by Kalkstein and Soven,¹ and a variety of related approaches have since been presented by a number of workers, including one of the present authors and collaborators (see Refs. 2–4, and references therein). Linear-chain mappings of surface and interfacial problems are a logical consequence of the two-dimensional periodicity retained in three-dimensional crystals when a cleavage or internal boundary plane is introduced, and may be applied to the following: electrons described by an orthogonal tight-binding Hamiltonian, phonons represented by a Born–von Kármán model, or magnons in the Heisenberg model. We will restrict our attention in this paper to the last of these. Alternative methods that may be used for such systems, but that we will not discuss further, include real-space recursion^{5–7} and slab calculations.⁸

The simple cubic lattice, with a single band and first-nearest-neighbor interactions only (sometimes referred to as cubium), has been studied in a number of papers for a variety of purposes. Because it is the simplest possible example, it is usually the sc (001) surface or interface that is considered. Kalkstein and Soven¹ illustrated their formalism with calculations for cubium. Dobrynski and Mills investigated vibrations of an adsorbed monolayer⁹ and reconstruction¹⁰ on the sc (001) surface. Einstein and Schrieffer¹¹ have looked at adsorbates and their interactions on cubium. Laks and Gonçalves da Silva¹² obtained the same results for the sc (001) surface as Kalkstein and Soven by using somewhat different methods. For magnons, DeWames and Wolfram¹³ showed that surface states below or above the bulk spectrum can occur with appropriate perturbations at the surface. Mills and Maradudin^{14,15} have discussed criteria for the existence of surface states in Heisenberg ferromagnets, and the effects of surfaces on thermodynamic properties thereof, using sc

(001) for illustrative results. Zhang¹⁶ has studied the formation of magnetic layers on nonmagnetic sc (001) substrates. Gumbs and Griffin¹⁷ and Weling¹⁸ have done Hubbard model calculations for surface magnetism at the cubium (001) surface. Yaniv has published work on both electronic states¹⁹ and spin waves²⁰ at sc (001) interfaces.

Similar calculations have been done for other crystals. Results have been presented for two-band models at (001) surfaces of CsCl- and NaCl-structure materials.^{21,22} Foo *et al.*²³ have applied what they call the effective-surface-potential method to the two-dimensional honeycomb lattice, Si(111), and the Bethe lattice. DeWames and Wolfram examined spin waves at sc (110) as well as sc (001) surfaces.¹³ The effects of surface steps have been investigated for electrons at fcc (111) and magnons at fcc (001) surfaces by Falicov and co-workers.^{24,25}

In the list of applications given in the preceding two

TABLE I. Blocking of single-band Hamiltonians at cubic surfaces and interfaces, with first- and second-nearest-neighbor interactions T_1 and T_2 , respectively. Where no entry is made in the column for $T_2=0$, i.e., for no second-nearest-neighbor interactions, the blocking is the same as for nonzero T_2 .

Crystal	Surface	$T_2 \neq 0$	$T_2 = 0$
sc	(001)	real, 1×1	
	(110)	real, 2×2	real, 1×1
	(111)	complex, 2×2	complex, 1×1
fcc	(001)	real, 2×2	real, 1×1
	(110)	real, 2×2	
	(111)	complex, 1×1	
bcc	(001)	real, 2×2	real, 1×1
	(110)	real, 1×1	
	(111)	complex, 3×3	
Zinc blende	(001)	real, 2×2	
	(110)	complex, 4×4	complex, 2×2
	(111)	complex, 2×2	

paragraphs, there appear few studies of the effects of crystal geometry and surface normal on surface and interface states in these simple systems. It is well known that the bulk densities of states for single bands in sc, fcc, and bcc crystals are quite different, and this might be expected to have some effect on the behavior at surfaces and interfaces. In this paper we present some results for spin waves at those surfaces and interfaces in cubic Heisenberg systems that can be described by the very simplest linear-chain mappings.

Table I shows the blocking of the Hamiltonian matrix, after transforming with respect to the two-dimensional wave vector, for the (001), (110), and (111) surfaces of sc, fcc, bcc, and zinc-blende crystals with first- and second-nearest-neighbor interactions. The detailed structure of the Hamiltonian transforms in the bulk for these systems is given in Appendix A. If only first-nearest-neighbor interactions are included, seven surfaces and interfaces exhibit 1×1 or scalar blocking, like linear chains with first-nearest-neighbor interactions: sc (001), (110), and (111); fcc (001) and (111); bcc (001) and (110). Analytic solutions for the Green's functions can readily be found for these cases, and it is these that we will discuss. The formalism is briefly reviewed in Sec. II. Illustrative results and some conclusions are presented in Sec. III.

II. MATHEMATICAL STRUCTURE

For magnons in cubic Heisenberg systems with first- and second-nearest-neighbor exchange, Table I shows that 1×1 or 2×2 blocking is the rule for (001), (110), and (111) surfaces and interfaces; the exceptions are bcc (111) and zinc-blende (110), and the latter reduces to 2×2 's if only first-nearest-neighbor interactions are included. We restrict our attention in this paper to those cases that block as 1×1 's, but because we consider perturbations that extend two layers on either side of the cleavage or interface plane we have used 2×2 blocking in many of our calculations.

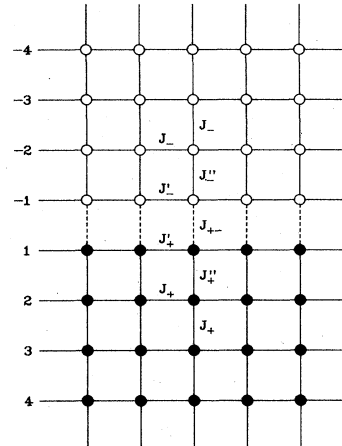


FIG. 1. Schematic drawing of the interface between two ferromagnetic half crystals with the same spin and first-nearest-neighbor exchange interactions. For surfaces, the interaction J_{+-} across the interface is set equal to zero.

The interfaces we consider consist of two semi-infinite lattices cut in the same way and in crystallographic registry with each other, which are brought together as shown in Fig. 1. For simplicity, only first-nearest-neighbor exchange is included. Interactions different from bulk values are allowed within the first plane and between the first and second planes on either side of the interface, as well as between the first planes on opposite sides. For surface calculations, the exchange interactions J_{+-} between the two half crystals are turned off. Yaniv²⁰ has recently done some work on spin waves at sc (001) interfaces in which only J_{+-} is allowed to differ from the bulk values J_+ and J_- , and we will from time to time draw some comparisons with this simpler model.

For 1×1 or scalar blocking, the two-dimensional transform of the Hamiltonian has the structure

$$\begin{array}{cccccc}
 H(-3, -3) & H(-3, -2) & 0 & 0 & 0 & 0 \\
 H(-2, -3) & \left[\begin{array}{ccc} H(-2, -2) & H(-2, -1) & 0 \\ H(-1, -2) & H(-1, -1) & H(-1, 1) \end{array} \right] & 0 & 0 & 0 \\
 0 & 0 & H(1, -1) & H(1, 1) & H(1, 2) & 0 \\
 0 & 0 & 0 & H(2, 1) & H(2, 2) & H(2, 3) \\
 0 & 0 & 0 & 0 & H(3, 2) & H(3, 3)
 \end{array} \quad (1)$$

Each element above is a function of the two-dimensional wave vector \mathbf{q}_s . According to our assumptions, elements within the large square brackets may differ from bulk values, those outside may not. Although we do not include changes in the intraplanar exchange interactions within planes $L = \pm 2$, $H(\pm 2, \pm 2)$ may be different from in the bulk because of the Goldstone rule, which requires that changes in non-site-diagonal terms in the Hamiltonian

in real space be accompanied by corresponding changes of opposite sign in the site-diagonal terms. For $L > 3$ we assume

$$H(\pm L, \pm L; \mathbf{q}_s) = A_{\pm}(\mathbf{q}_s), \quad (2)$$

$$H(\pm(L-1), \pm L; \mathbf{q}_s) = B_{\pm}(\mathbf{q}_s). \quad (3)$$

The two semi-infinite crystals are uncoupled if we set

$0=H(\pm 1, \mp 1; \mathbf{q}_s)$. Note that there is no plane 0 in our notation. Details of the spin-wave Hamiltonian transforms in the interfacial region for the various crystals and directions considered in this paper are given in Appendix B. Yaniv²⁰ studied only sc (001), and allowed only $H(\pm 1, \mp 1)$ [and $H(\pm 1, \pm 1)$ through the Goldstone rule] to differ from bulk values.

Using the methods outlined in Refs. 2–4, it is straightforward to derive expressions for the Green's functions in the surface and interface regions. First, by following a sequence of recursion equations until they begin to repeat, terminated-bulk Green's functions $g_{\pm}(\mathbf{q}_s; z)$ are defined by

$$g_{\pm} = \frac{1}{2|B_{\pm}|^2} \{z - A_{\pm} - [(z - A_{\pm})^2 - 4|B_{\pm}|^2]^{1/2}\}, \quad (4)$$

where the proper choice of branch for the square root is that for which $g_{\pm} \rightarrow 1/E$ for $z = E \rightarrow \pm \infty$ and $\text{Im}[g_{\pm}(z = E + i0+)] < 0$. These are the Green's functions for the first layers of two half crystals in which all elements of the Hamiltonian transforms retain their bulk values. For magnons, this is not equivalent to cleavage, because the Goldstone rule is not obeyed in what we refer to as the terminated-bulk crystal.

Consider, for example, the sc (001) surface with first-nearest-neighbor exchange J only. From Appendices A and B the Hamiltonian transforms in the bulk are

$$H(L, L; \mathbf{q}_s) = A(\mathbf{q}_s) = J\{6 - 2[\cos(2\pi\xi_1) + \cos(2\pi\xi_2)]\}, \quad (5a)$$

$$H(L, L+1; \mathbf{q}_s) = B(\mathbf{q}_s) = -J, \quad (5b)$$

where $\mathbf{q}_s = (2\pi/a)\xi$. For $\mathbf{q}_s \rightarrow 0$, these obey the bulk Goldstone rule

$$0 = H(L, L; 0) + H(L, L+1; 0) + H(L, L-1; 0). \quad (6)$$

In what we call the terminated-bulk crystal, the Hamiltonian in the surface plane is $H(1, 1; \mathbf{q}_s) = A(\mathbf{q}_s)$, the same as in the bulk. This is different from the first-plane Hamiltonian transform for a proper cleaved crystal, with no changes in the exchange interactions. At the cleaved sc (001) surface, spins in the first layer $L=1$ interact with four other spins in the same layer and with one in plane $L=2$, but not with a spin in $L=-1$. The Hamiltonian transform for the surface plane in the cleaved crystal is therefore reduced by one exchange interaction from its bulk value,

$$H(1, 1; \mathbf{q}_s) = J\{5 - 2[\cos(2\pi\xi_1) + \cos(2\pi\xi_2)]\}, \quad (7)$$

and the Goldstone rule for the surface layer is

$$0 = H(1, 1; 0) + H(1, 2; 0). \quad (8)$$

Returning from this brief digression to the more general problem, the Green's functions for the first two layers at the surface or interface may be expressed in terms of the Hamiltonian transform elements and the terminated-bulk Green's functions. Suppressing the arguments \mathbf{q}_s and z , the surface Green's functions are

$$G^{\pm\pm} = \frac{1}{D_{\pm}} \begin{bmatrix} z - H(\pm 2, \pm 2) - |B_{\pm}|^2 g_{\pm} & H^*(\pm 1, \pm 2) \\ H(\pm 1, \pm 2) & z - H(\pm 1, \pm 1) \end{bmatrix}, \quad (9)$$

$$D_{\pm} = [z - H(\pm 1, \pm 1)][z - H(\pm 2, \pm 2) - |B_{\pm}|^2 g_{\pm}] - |H(\pm 1, \pm 2)|^2. \quad (10)$$

For the first two planes on either side of the interface, we obtain

$$\Gamma^{\pm\pm} = \frac{1}{\Delta_{\pm}} \begin{bmatrix} z - H(\pm 2, \pm 2) - |B_{\pm}|^2 g_{\pm} & H^*(\pm 1, \pm 2) \\ H(\pm 1, \pm 2) & z - H(\pm 1, \pm 1) - |H(\pm 1, -1)|^2 G_{11}^{\mp\mp} \end{bmatrix}, \quad (11)$$

$$\Delta_{\pm} = [z - H(\pm 1, \pm 1) - |H(\pm 1, -1)|^2 G_{11}^{\mp\mp}][z - H(\pm 2, \pm 2) - |B_{\pm}|^2 g_{\pm}] - |H(\pm 1, \pm 2)|^2, \quad (12)$$

where $G_{11}^{\mp\mp}$ is the 11 element of the 2×2 matrix in Eq. (9). Note that if $H(\pm 1, \mp 1)$ is set equal to zero in Eqs. (11) and (12) for the interface, that is, if the interactions between the two half crystals are severed, the surface results in Eqs. (9) and (10) are recovered.

III. RESULTS

True surface and interface states occur at energies outside the bulk spectrum as isolated poles of the Green's functions with nonzero residues for some or all surface wave vectors \mathbf{q}_s . In our model they arise at zeros of the denominators D_{\pm} and Δ_{\pm} in Eqs. (10) and (12). Integration over the surface Brillouin zone (SBZ) yields surface or interface densities of states for excitations in the various layers.

From Eq. (4), it is clear that no surface states occur for

what we call the terminated bulk, a half crystal in which all elements of the Hamiltonian retain their bulk values. The terminated-bulk Green's function has two branch points, but no isolated poles. The bulk intraplanar Green's function

$$G_0(z) = G_0(L, L; z) = \frac{1}{[(z - A)^2 - 4|B|^2]^{1/2}} \quad (13)$$

also has no poles, but only branch points at the bulk band edges

$$E_{\pm}(\mathbf{q}_s) = A(\mathbf{q}_s) \pm 2|B(\mathbf{q}_s)|, \quad (14)$$

the same points as for the terminated bulk.

To illustrate the formation of surface and interface states, we first consider the very simplest example, namely the case where only the outermost surface layer or a single interfacial plane differs from the bulk. The Hamiltonian

transform in this one plane is

$$A_1(\mathbf{q}_s) = H(1, 1; \mathbf{q}_s), \quad (15)$$

and all other elements of the transforms are

$$A(\mathbf{q}_s) = H(L, L; \mathbf{q}_s), \quad (16)$$

$$B(\mathbf{q}_s) = H(L, L + 1; \mathbf{q}_s). \quad (17)$$

When A_1 differs from A , a surface state may form, provided that the condition

$$(A_1 - A)^2 - |B|^2 > 0 \quad (18)$$

is satisfied, and an interface state is formed regardless of the size of the perturbation (so long as $A_1 \neq A$). The surface-state energy E_S , residue in the first plane R_S , and total surface-state density of states σ_S in the first layer are, respectively,

$$E_S = E_- + A_1 - A + 2|B| + \frac{|B|^2}{A_1 - A}, \quad (19a)$$

$$R_S = 1 - \frac{|B|^2}{(A_1 - A)^2}, \quad (19b)$$

$$\sigma_S = \frac{1}{A_{\text{SBZ}}} \int_{\text{SBZ}} R_S, \quad (19c)$$

where A_{SBZ} is the area of the SBZ. For an interface for which $A_1 \neq A$, the interface-state energy, residue, and total interface-state density of states (in the interfacial plane) are

$$E_I = A + [(A_1 - A)^2 + 4|B|^2]^{1/2} \text{sgn}(A_1 - A), \quad (20a)$$

$$R_I = \frac{|A_1 - A|}{[(A_1 - A)^2 + 4|B|^2]^{1/2}}, \quad (20b)$$

$$\sigma_I = \frac{1}{A_{\text{SBZ}}} \int_{\text{SBZ}} R_I. \quad (20c)$$

Note that the residues in Eqs. (19b) and (20b), and hence also the total densities of states in Eqs. (19c) and (20c), are less than 1, as they must be.

This simple example considered above applies to magnons in cleaved Heisenberg systems for which 1×1 blocking occurs. If there are no changes in the nearest-neighbor exchange interactions in the surface region, then the only change in the Hamiltonian transforms arises from the Goldstone rule, that is, from the fact that in the surface layer a spin has fewer neighbors than in the bulk. The perturbation is

$$A_1 - A = -(Z - Z_1)J, \quad (21)$$

where J is the first-nearest-neighbor exchange interaction, and Z and $Z_1 < Z$ are the coordination numbers for spins in the bulk and in the surface layer, respectively.

For the seven cubic crystal surfaces that exhibit 1×1 blocking (see Table I and Appendix B), cleavage and the Goldstone rule by themselves have several interesting effects. First, they produce no surface states for magnons at the sc (001) surface, because $A_1 - A = B = -J$; the inequality (18) is not satisfied, and from Eqs. (19a) and (19b) the would-be surface state falls at the bottom of the

bulk band with zero residue, $E_S = E_-$ and $R_S = 0$. The absence of surface states for cleaved sc (001) with first-nearest-neighbor exchange only was pointed out by Mills and Maradudin¹⁴ as an example of a somewhat more general conclusion: If cleavage severs only bonds normal to the surface (and the exchange interactions in the surface region retain their bulk values otherwise), surface states do not occur. Surface spin-wave states will be found if cleavage cuts bonds that are not perpendicular to the surface, and this is confirmed for the other six surfaces studied here. The surface-state energies relative to the bottom of the bulk band, $E_S - E_-$, the residues R_S , and the integrated densities of states σ_S turn out to be independent of the underlying crystal structure, and depend only on the surface normal. The surface states are weakest for sc (110) and bcc (110) ($\sigma_S = \frac{1}{2}$), stronger for sc (111) and bcc (111) ($\sigma_S = \frac{2}{3}$), and strongest for fcc (001) and bcc (001) ($\sigma_S = \frac{3}{4}$).

Although $E_S - E_-$ and R_S have the same functional form for the above pairs of crystals with the same surface normals, the lower bulk band limits E_- and hence the surface-state energies E_S do depend on the crystal structure. For the fcc and bcc (001) surfaces, for example, we find, upon working through the details [cf. Eqs. (14), (19a), (19b), and (21), and Appendices A and B] that

$$E_S - E_- = -4J[1 - \cos(\pi\xi_1)\cos(\pi\xi_2)]^2, \quad (22a)$$

$$R_S = 1 - \cos^2(\pi\xi_1)\cos^2(\pi\xi_2), \quad (22b)$$

but the lower bulk band limits are

$$E_- = 4J\{4 - [\cos(\pi\xi_1) + \cos(\pi\xi_2)]^2\} \quad (23)$$

for fcc (001), and

$$E_- = 8J[1 - \cos(\pi\xi_1)\cos(\pi\xi_2)] \quad (24)$$

for bcc (001). Because of this difference the surface-state densities of states will be quite different for the two surfaces.

Figures 2–4 show bulk, terminated-bulk, and cleaved-surface-layer densities of states for the sc (110), fcc (001), and bcc (001) surfaces, respectively, assuming a first-nearest-neighbor exchange interaction $J = 1$. The band-state contributions to the plane-1 totals for the cleaved crystals are shown as dashed lines. All results are obtained by summation over large numbers of evenly spaced points in the irreducible SBZ's for the various crystal faces, e.g., over 20 100 points for the bulk and (001) terminated-bulk fcc and bcc densities of states, and over 80 200 points for the surface states. A small amount of noise is evident in the curves, particularly for the bulk, even with such fine integration meshes.

As previously remarked, the bulk densities of states are quite different for the three crystal structures. The effects of the Goldstone rule appear as dramatic differences between the terminated-bulk results and the plane-1 densities of states for the cleaved crystals. In this regard, we note that the terminated-bulk curves correspond to perhaps the simplest possible model for electronic states at surfaces, one in which all elements of the Hamiltonian in a half crystal retain the bulk values.

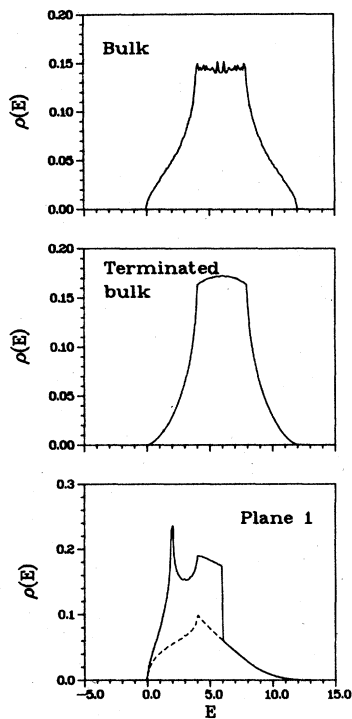


FIG. 2. Bulk, terminated-bulk, and cleaved-crystal (plane 1) densities of states for magnons at sc (110), for $J=1$. The dashed line in the bottom panel gives the band-state contributions for plane 1 in the cleaved crystal.

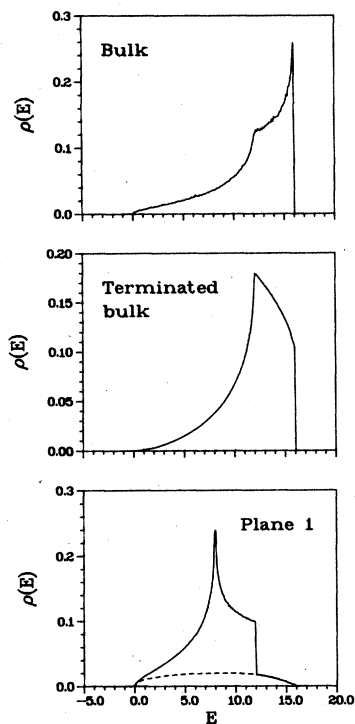


FIG. 3. Bulk, terminated-bulk, and cleaved-crystal (plane 1) densities of states for fcc (001).

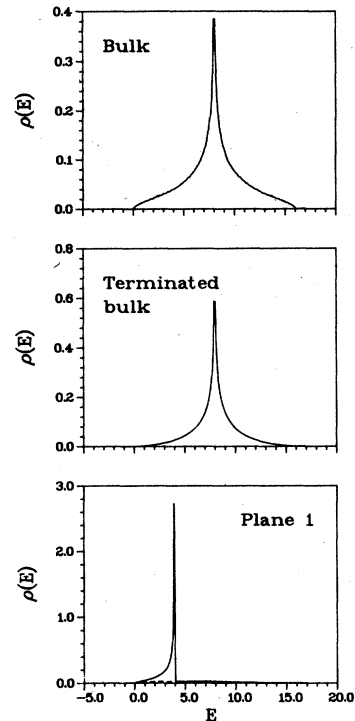


FIG. 4. Bulk, terminated-bulk, and cleaved-crystal (plane 1) densities of states for bcc (001).

The impact of the underlying crystal structure on excitations at surfaces is illustrated by the quite different results obtained for the (001) surfaces of fcc and bcc crystals in Figs. 3 and 4. We recall here that for the cleaved sc (001) surface there are no surface states at all, while for fcc and bcc (001) they contribute 75% of the total density of states in the surface layer. For a given crystal structure, variation from one surface to another may produce differences just as striking, as is attested by a comparison between the bottom panel of Fig. 4 for bcc (001) and Fig. 5 for bcc (110).

For the results described above, 1×1 blocking was used throughout the calculations, and the imaginary part of the energy was set equal to zero ($z = E + i0+$). For the somewhat more general situation shown in Fig. 1, the per-

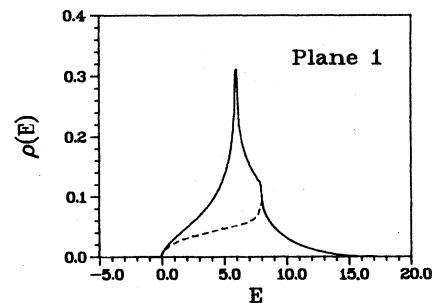


FIG. 5. Plane-1 densities of states at the cleaved bcc (110) surface.

turbations extend into two layers in the surface region or on either side of the interface, rather than being confined to a single surface or interface plane. For this case, there is some conceptual convenience in using 2×2 blocking,³ even though the Hamiltonian transform matrices of course retain the 1×1 structure shown in Appendix B. This conceptual simplification is gained at the cost of increased computational complexity, however, as 2×2 matrices rather than scalars must be manipulated. For density-of-states calculations, we therefore add a small imaginary part to the energy to keep computer-time expenditures within reasonable limits; for the calculations discussed below, $\text{Im}z = 0.04$. This produces some rounding of singularities and tailing at upper and lower spectral limits.

The examples we will consider will be surfaces or symmetric interfaces, where by the latter we mean that the exchange interactions in the two half crystals are mirror images. The notation for the exchange interactions in Fig. 1 and Appendix B can be simplified accordingly, as follows: bulk, $J = J_+ = J_-$; across the interface J_{+-} ; within planes ± 1 , $J' = J'_+ = J'_-$; between planes ± 1 and ± 2 , $J'' = J''_+ = J''_-$.

The effects of increasing the range of the perturbations at an interface are illustrated in Fig. 6 for sc (001). The top panel is for Yaniv's model,²⁰ in which all exchange interactions have the same value except for those connecting the first planes in the two half crystals. Yaniv concluded for this case that there will be interface states only if $J_{+-} > J$. With the parameters chosen for Fig. 6(a)

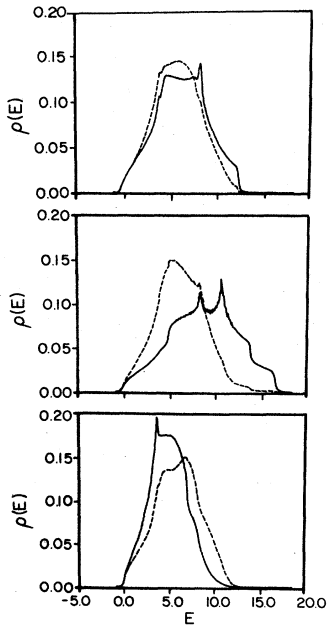


FIG. 6. Total densities of states for planes ± 1 (solid lines) and ± 2 (dashed lines) at sc (001) interfaces. In this and all subsequent figures the exchange interaction in the bulk is taken to be $J = 1$. Values for the other parameters here are as follows: top panel, $J_{+-} = 1.5$ and $J' = J'' = 1$; middle panel, $J_{+-} = J' = 1.5$ and $J'' = 1.3$; bottom panel, $J_{+-} = J' = 0.8$ and $J'' = 0.9$.

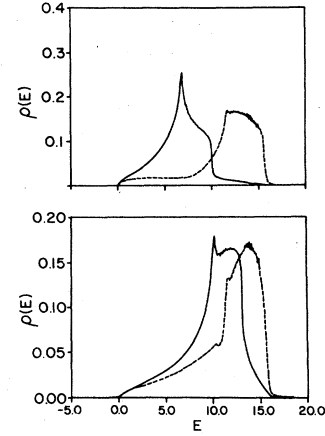


FIG. 7. Surface (top) and interface (bottom) densities of states for planes 1 and 2 for fcc (001), with $J' = 0.8$ and $J'' = 0.9$, and for the interface, $J_{+-} = 0.8$.

($J_{+-} = 1.5$, $J = J' = J'' = 1.0$), interface states are apparent, since the densities of states in planes ± 1 and ± 2 extend somewhat above the bulk band limit of 12. If we extend the range of the perturbations, the interface states shift and change in intensity, as shown in Fig. 6(b). For these results the interactions in planes ± 1 were also given the value $J' = 1.5$, and the coupling between the first and second layers was increased by a somewhat smaller amount, $J'' = 1.3$. The spectral density has shifted to higher energies, particularly for planes ± 1 , and the contribution of the interface states to the total has increased; for plane 1, the integrated density of states defined in Eq. (20c) is $\sigma_1 = 0.38$ for Fig. 6(a) and $\sigma_1 = 0.67$ for Fig. 6(b).

With perturbations of longer range than in Yaniv's model, it is also possible for interface states to form in certain cases if the interactions in the interfacial region are weaker than in the bulk, rather than stronger. Figure 6(c) shows the total densities of states in planes 1 and 2 for one such example. Calculations of the Green's func-

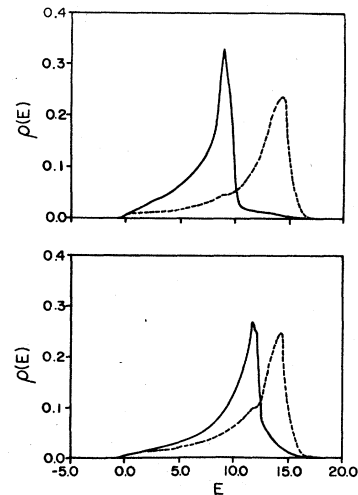


FIG. 8. Surface (top) and interface (bottom) densities of states for fcc (111), with the same parameters as in Fig. 7.

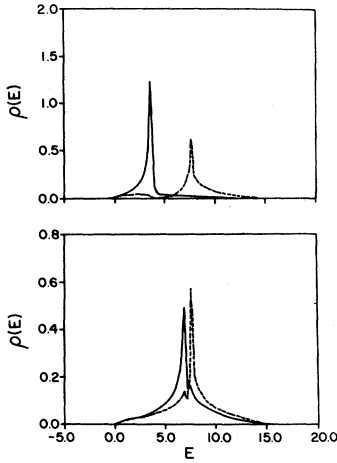


FIG. 9. Surface (top) and interface (bottom) densities of states for bcc (001), with the same parameters as in Fig. 7.

tions for particular surface wave vectors indicate that interface states split off below the bulk bands for this set of parameters ($J = 1.0$, $J_{+-} = J' = 0.8$, $J'' = 0.9$), and contribute to the peaks in the curves of Fig. 6(c) at $E \sim 4$.

As for surface spin waves in cleaved crystals, it turns out that sc (001) is the least interesting subject for study in Yaniv's simple model for a bicrystal. For all of the other six interfaces with 1×1 blocking, interface states occur for any change in the exchange interactions across the interface. For $J_{+-} > J$, one interface state splits off above the band states at all surface wave vectors, and a second, also above the bulk band, exists at selected wave vectors. For $J_{+-} < J$, the same occurs, but with both interface states below the bulk states.

To illustrate the effects of crystal structure and surface normal with the more extensive perturbations in Fig. 1, Figs. 7–10 show total densities of states for the first two planes at fcc (001) and (111) and bcc (001) and (110) surfaces and interfaces. All calculations were done with the same set of parameters used for Fig. 6(c), corresponding to a modest weakening of the exchange interactions in the surface or interfacial region. These parameters were not chosen to be representative of any particular system, because of a lack of such information experimentally. From neutron-scattering experiments on the bulk, it is known, for example, that the europium chalcogenides EuO, EuS, EuSe, and EuTe fit the Heisenberg description.²⁶ There has been some discussion of surface spin waves and magnetic reconstruction in these materials,²⁷ but no definitive values for the exchange interactions have been found.

We do not wish to dwell on the detailed structure in Figs. 7–10, but we will make a few comments on some general features of the results. First, and not really obvious in these total density-of-states curves, surface or interface states occur in all instances, split off below the bulk bands for any given surface wave vector. Second, as expected, interfaces introduce weaker perturbations than surfaces, because interactions are only altered rather than severed. Third, "healing" back toward the bulk spectral densities (cf. Figs. 2–4) takes place fairly rapidly. Final-

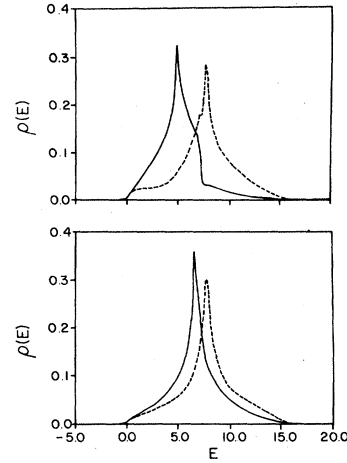


FIG. 10. Surface (top) and interface (bottom) densities of states for bcc (110), with the same parameters as in Fig. 7.

ly, there are quite pronounced differences in the results for different faces of the same crystal, and in those for the same face of different crystals. As we noted at the outset, sc (001) has been used as an example in many studies of elementary excitations at surfaces and interfaces, even though it now appears in retrospect to be the least interesting case that could be chosen.

ACKNOWLEDGMENTS

The authors are grateful to C. Y. Huang and S. H. Liu for helpful conversations. This research was sponsored by the Division of Materials Science, U. S. Department of Energy, under Contract No. DE-AC05-84OR21400 with Martin Marietta Energy Systems, Inc.

APPENDIX A: BULK HAMILTONIAN TRANSFORMS

This appendix gives the detailed structure of the two-dimensional transforms of the bulk, single-band Hamiltonians for cubic crystals with a site-diagonal element E and first- and second-nearest-neighbor interactions T_1 and T_2 . For spin waves in Heisenberg systems, the first- and second-nearest-neighbor interactions T_i are identified as exchange interactions J_i , and the Goldstone rule specifies the site-diagonal term E ,

$$E = Z_1 J_1 + Z_2 J_2, \quad (\text{A1})$$

where Z_1 and Z_2 are the numbers of first- and second-nearest-neighbors.

1. Simple cubic

For the sc (001) surface, we have

$$\mathbf{q}_s = (2\pi/a)(\xi_1, \xi_2, 0),$$

$$H(L, L; \mathbf{q}_s) = E + 2T_1 [\cos(2\pi\xi_1) + \cos(2\pi\xi_2)] + 4T_2 \cos(2\pi\xi_1) \cos(2\pi\xi_2),$$

$$H(L, L+1; \mathbf{q}_s) = T_1 + 2T_2 [\cos(2\pi\xi_1) + \cos(2\pi\xi_2)] .$$

For the sc (110),

$$\mathbf{q}_s = (\pi/a)(\xi_2, -\xi_2, 2\xi_1) ,$$

$$H(L, L; \mathbf{q}_s) = E + 2T_1 \cos(2\pi\xi_1) + 2T_2 \cos(2\pi\xi_2) ,$$

$$H(L, L+1; \mathbf{q}_s) = 2 \cos(\pi\xi_2) [T_1 + 2T_2 \cos(2\pi\xi_1)] ,$$

$$H(L, L+2; \mathbf{q}_s) = T_2 .$$

For the sc (111),

$$\mathbf{q}_s = (2\pi/3a)(-2\xi_1 - \xi_2, \xi_1 - \xi_2, \xi_1 + 2\xi_2) ,$$

$$H(L, L; \mathbf{q}_s) = E + 2T_2 \{ \cos(2\pi\xi_1) + \cos(2\pi\xi_2) \\ + \cos[2\pi(\xi_1 + \xi_2)] \} ,$$

$$H(L, L+1; \mathbf{q}_s) = T_1 e^{-(2\pi i/3)(\xi_1 - \xi_2)} (1 + e^{2\pi i \xi_1} + e^{-2\pi i \xi_2}) ,$$

$$H(L, L+2; \mathbf{q}_s) = T_2 e^{(2\pi i/3)(\xi_1 - \xi_2)} (1 + e^{-2\pi i \xi_1} + e^{2\pi i \xi_2}) .$$

2. Face-centered cubic

For the fcc (001) surface, we have

$$\mathbf{q}_s = (2\pi/a)(\xi_1 + \xi_2, -\xi_1 + \xi_2, 0) ,$$

$$H(L, L; \mathbf{q}_s) = E + 2T_1 [\cos(2\pi\xi_1) + \cos(2\pi\xi_2)] \\ + 4T_2 \cos(2\pi\xi_1) \cos(2\pi\xi_2) ,$$

$$H(L, L+1; \mathbf{q}_s) = 4T_1 \cos(\pi\xi_1) \cos(\pi\xi_2) ,$$

$$H(L, L+2; \mathbf{q}_s) = T_2 .$$

For the fcc (110),

$$\mathbf{q}_s = (2\pi/a)(\xi_2, -\xi_2, 2\xi_1) ,$$

$$H(L, L; \mathbf{q}_s) = E + 2T_1 \cos(2\pi\xi_2) + 2T_2 \cos(2\pi\xi_1) ,$$

$$H(L, L+1; \mathbf{q}_s) = 4T_1 \cos(\pi\xi_1) \cos(\pi\xi_2) ,$$

$$H(L, L+2; \mathbf{q}_s) = T_1 + 2T_2 \cos(2\pi\xi_2) .$$

For the fcc (111),

$$\mathbf{q}_s = (4\pi/3a)(-2\xi_1 - \xi_2, \xi_1 - \xi_2, \xi_1 + 2\xi_2) ,$$

$$H(L, L; \mathbf{q}_s) = E + 2T_1 \{ \cos(2\pi\xi_1) + \cos(2\pi\xi_2) \\ + \cos[2\pi(\xi_1 + \xi_2)] \} ,$$

$$\mathbf{q}_s = (2\pi/a)(\xi_1 + \xi_2, -\xi_1 + \xi_2, 0) ,$$

$$H(LA, LA; \mathbf{q}_s) = E^A + 2T_2^{AA} [\cos(2\pi\xi_1) + \cos(2\pi\xi_2)] ,$$

$$H((L+1)B, (L+1)B; \mathbf{q}_s) = E^B + 2T_2^{BB} [\cos(2\pi\xi_1) + \cos(2\pi\xi_2)] ,$$

$$H(LA, (L+1)B; \mathbf{q}_s) = 2T_1 \cos(\pi\xi_1) ,$$

$$H((L+1)B, (L+2)A; \mathbf{q}_s) = 2T_1 \cos(\pi\xi_2) ,$$

$$H(LA, (L+2)A; \mathbf{q}_s) = 4T_2^{AA} \cos(\pi\xi_1) \cos(\pi\xi_2) ,$$

$$H((L+1)B, (L+3)B; \mathbf{q}_s) = 4T_2^{BB} \cos(\pi\xi_1) \cos(\pi\xi_2) .$$

For the zinc-blende (110) surface,

$$H(L, L+1; \mathbf{q}_s) = T_1 e^{(2\pi i/3)(\xi_1 - \xi_2)} (1 + e^{-2\pi i \xi_1} + e^{2\pi i \xi_2}) \\ + T_2 e^{-(4\pi i/3)(\xi_1 - \xi_2)} \\ \times (1 + e^{4\pi i \xi_1} + e^{-4\pi i \xi_2}) .$$

3. Body-centered cubic

For the bcc (001) surface, we have

$$\mathbf{q}_s = (2\pi/a)(\xi_1, \xi_2, 0) ,$$

$$H(L, L; \mathbf{q}_s) = E + 2T_2 [\cos(2\pi\xi_1) + \cos(2\pi\xi_2)] ,$$

$$H(L, L+1; \mathbf{q}_s) = 4T_1 \cos(\pi\xi_1) \cos(\pi\xi_2) ,$$

$$H(L, L+2; \mathbf{q}_s) = T_2 .$$

For the bcc (110),

$$\mathbf{q}_s = (\pi/a)(\xi_1 + 2\xi_2, -\xi_1 - 2\xi_2, 2\xi_1) ,$$

$$H(L, L; \mathbf{q}_s) = E + 2T_1 \{ \cos(2\pi\xi_2) + \cos[2\pi(\xi_1 + \xi_2)] \} \\ + 2T_2 \cos(2\pi\xi_1) ,$$

$$H(L, L+1; \mathbf{q}_s) = 2T_1 \cos(\pi\xi_1) + 2T_2 \cos[\pi(\xi_1 + 2\xi_2)] .$$

For the bcc (111),

$$\mathbf{q}_s = (2\pi/3a)(-2\xi_1 - \xi_2, \xi_1 - \xi_2, \xi_1 + 2\xi_2) ,$$

$$H(L, L; \mathbf{q}_s) = E ,$$

$$H(L, L+1; \mathbf{q}_s) = T_1 e^{(2\pi i/3)(\xi_1 - \xi_2)} (1 + e^{-2\pi i \xi_1} + e^{2\pi i \xi_2}) ,$$

$$H(L, L+2; \mathbf{q}_s) = T_2 e^{-(2\pi i/3)(\xi_1 - \xi_2)} (1 + e^{2\pi i \xi_1} + e^{-2\pi i \xi_2}) ,$$

$$H(L, L+3; \mathbf{q}_s) = T_1 .$$

4. Zinc blende

In the zinc-blende lattice, there are two types of atoms in general, which we label A and B , and they occupy different sublattices that are not equivalent even when atoms A and B are the same. For the [110] surface-normal direction, any plane L contains equal numbers of atoms belonging to both sublattices, while for the [001] and [111] directions the atoms in any given plane belong wholly to one sublattice or the other, which alternate from plane to plane.

For the zinc-blende (001) surface,

$$\begin{aligned}
\mathbf{q}_s &= (2\pi/a)(\xi_2, -\xi_2, 2\xi_1), \\
H(Li, Li; \mathbf{q}_s) &= E^i + 2T_2^{ii} \cos(2\pi\xi_2), \\
H(LA, LB; \mathbf{q}_s) &= 2T_1 e^{-\pi i \xi_1} \cos(\pi\xi_2), \\
H(Li, (L+1)i; \mathbf{q}_s) &= 4T_2^{ii} \cos(2\pi\xi_1) \cos(\pi\xi_2), \\
H(LA, (L+1)B; \mathbf{q}_s) &= T_1 e^{\pi i \xi_1}, \\
H(Li, (L+2)i; \mathbf{q}_s) &= T_2^{ii}.
\end{aligned}$$

For the zinc-blende (111) surface,

$$\begin{aligned}
\mathbf{q}_s &= (4\pi/3a)(-2\xi_1 - \xi_2, \xi_1 - \xi_2, \xi_1 + 2\xi_2), \\
H(LA, LA; \mathbf{q}_s) &= E^A + 2T_2^{AA} \{ \cos(2\pi\xi_1) + \cos(2\pi\xi_2) + \cos[2\pi(\xi_1 + \xi_2)] \}, \\
H((L+1)B, (L+1)B; \mathbf{q}_s) &= E^B + 2T_2^{BB} \{ \cos(2\pi\xi_1) + \cos(2\pi\xi_2) + \cos[2\pi(\xi_1 + \xi_2)] \}, \\
H(LA, (L+1)B; \mathbf{q}_s) &= T_1 e^{(2\pi i/3)(\xi_1 - \xi_2)} (1 + e^{-\pi i \xi_1} + e^{\pi i \xi_2}), \\
H((L+1)B, (L+2)A; \mathbf{q}_s) &= T_1, \\
H(LA, (L+2)A; \mathbf{q}_s) &= T_2^{AA} e^{(2\pi i/3)(\xi_1 - \xi_2)} (1 + e^{-\pi i \xi_1} + e^{\pi i \xi_2}), \\
H((L+1)B, (L+3)B; \mathbf{q}_s) &= T_2^{BB} e^{(2\pi i/3)(\xi_1 - \xi_2)} (1 + e^{-\pi i \xi_1} + e^{\pi i \xi_2}),
\end{aligned}$$

APPENDIX B: INTERFACE SPIN-WAVE HAMILTONIANS

In this appendix we give the elements of the Hamiltonian transforms for magnons in the four-plane interfacial region ($L = -2, -1, 1, 2$) in which we allow $H(L, L'; \mathbf{q}_s)$ to differ from the bulk values. More specifically, we provide the block of the Hamiltonian transform that is enclosed in large square brackets in Eq. (1),

$$H_I(\mathbf{q}_s) = \begin{bmatrix} H(-2, -2; \mathbf{q}_s) & H(-2, -1; \mathbf{q}_s) & 0 & 0 \\ H(-1, -2; \mathbf{q}_s) & H(-1, -1; \mathbf{q}_s) & H(-1, 1; \mathbf{q}_s) & 0 \\ 0 & H(1, -1; \mathbf{q}_s) & H(1, 1; \mathbf{q}_s) & H(1, 2; \mathbf{q}_s) \\ 0 & 0 & H(2, 1; \mathbf{q}_s) & H(2, 2; \mathbf{q}_s) \end{bmatrix}, \quad (\text{B1})$$

for the seven cases for which 1×1 blocking occurs. For simplicity, only first-nearest-neighbor exchange is included in all cases; the nearest-neighbor exchange interactions in the upper and lower bulk crystals are denoted by J_+ and J_- , respectively.

For the sc (001) surface, we have

$$\begin{aligned}
C &= 2[\cos(2\pi\xi_1) + \cos(2\pi\xi_2)], \\
H &= \begin{bmatrix} 5J_- + J_-'' - J_- C & -J_-'' & 0 & 0 \\ -J_-'' & 4J_- + J_-'' + J_{+-} - J_- C & -J_{+-} & 0 \\ 0 & -J_{+-} & 4J_+ + J_+'' + J_{+-} - J_+ C & -J_+'' \\ 0 & 0 & -J_+'' & 5J_+ + J_+'' - J_+ C \end{bmatrix}.
\end{aligned}$$

For the sc (110),

$$\begin{aligned}
C_1 &= 2 \cos(2\pi\xi_1), \quad C_2 = 2 \cos(\pi\xi_2), \\
H &= \begin{bmatrix} 4J_- + 2J_-'' - J_- C_1 & -J_-'' C_2 & 0 & 0 \\ -J_-'' C_2 & 2(J_- + J_-'' + J_{+-}) - J_- C_1 & -J_{+-} C_2 & 0 \\ 0 & -J_{+-} C_2 & 2(J_+ + J_+'' + J_{+-}) - J_+ C_1 & -J_+'' C_2 \\ 0 & 0 & -J_+'' C_2 & 4J_+ + 2J_+'' - J_+ C_1 \end{bmatrix}.
\end{aligned}$$

For the sc (111),

$$C = e^{-(2\pi i/3)(\xi_1 - \xi_2)} (1 + e^{2\pi i \xi_1} + e^{-2\pi i \xi_2}),$$

$$H = \begin{bmatrix} 3J_- + 3J'' & -J''C & 0 & 0 \\ -J''C^* & 3J'' + 3J_{+-} & -J_{+-}C & 0 \\ 0 & -J_{+-}C^* & 3J'' + 3J_{+-} & -J''C \\ 0 & 0 & -J''C^* & 3J_{+-} + 3J'' \end{bmatrix}.$$

For the fcc (001),

$$C_1 = 2[\cos(2\pi\xi_1) + \cos(2\pi\xi_2)], \quad C_2 = 4 \cos(\pi\xi_1) \cos(\pi\xi_2),$$

$$H = \begin{bmatrix} 8J_- + 4J'' - J_-C_1 & -J''C_2 & 0 & 0 \\ -J''C_2 & 4(J'_- + J''_- + J_{+-}) - J'_-C_1 & -J_{+-}C_2 & 0 \\ 0 & -J_{+-}C_2 & 4(J'_+ + J''_+ + J_{+-}) - J'_+C_1 & -J''_+C_2 \\ 0 & 0 & -J''_+C_2 & 8J_+ + 4J''_+ - J_+C_1 \end{bmatrix}.$$

For the fcc (111),

$$C_1 = 2\{\cos(2\pi\xi_1) + \cos(2\pi\xi_2) + \cos[2\pi(\xi_1 + \xi_2)]\}, \quad C_2 = e^{(2\pi i/3)(\xi_1 - \xi_2)} (1 + e^{-2\pi i \xi_1} + e^{2\pi i \xi_2}),$$

$$H = \begin{bmatrix} 9J_- + 3J'' - J_-C_1 & -J''C_2 & 0 & 0 \\ -J''C_2^* & 6J'_- + 3J''_- + 3J_{+-} - J'_-C_1 & -J_{+-}C_2 & 0 \\ 0 & -J_{+-}C_2^* & 6J'_+ + 3J''_+ + 3J_{+-} - J'_+C_1 & -J''_+C_2 \\ 0 & 0 & -J''_+C_2^* & 9J_+ + 3J''_+ - J_+C_1 \end{bmatrix}.$$

For the bcc (001),

$$C = 4 \cos(\pi\xi_1) \cos(\pi\xi_2),$$

$$H = \begin{bmatrix} 4J_- + 4J'' & -J''C & 0 & 0 \\ -J''C & 4J'' + 4J_{+-} & -J_{+-}C & 0 \\ 0 & -J_{+-}C & 4J'' + 4J_{+-} & -J''C \\ 0 & 0 & -J''C & 4J_{+-} + 4J'' \end{bmatrix}.$$

For the bcc (110),

$$C_1 = 2\{\cos(2\pi\xi_2) + \cos[2\pi(\xi_1 + \xi_2)]\}, \quad C_2 = 2 \cos(\pi\xi_1),$$

$$H = \begin{bmatrix} 6J_- + 2J'' - J_-C_1 & -J''C_2 & 0 & 0 \\ -J''C_2 & 4J'_- + 2J''_- + 2J_{+-} - J'_-C_1 & -J_{+-}C_2 & 0 \\ 0 & -J_{+-}C_2 & 4J'_+ + 2J''_+ + 2J_{+-} - J'_+C_1 & -J''_+C_2 \\ 0 & 0 & -J''_+C_2 & 6J_+ + 2J''_+ - J_+C_1 \end{bmatrix}.$$

*On leave from the Institute of Physics, The Chinese Academy of Sciences, Beijing, China.

†Permanent address: Department of Physics and Astronomy, Louisiana State University, Baton Rouge, LA 70803.

¹D. Kalkstein and P. Soven, *Surf. Sci.* **26**, 85 (1971).

²M. Mostoller and T. Kaplan, *Phys. Rev. B* **19**, 552 (1978).

³M. Mostoller and A. K. Rajagopal, *Phys. Rev. B* **25**, 6168 (1982).

⁴M. Mostoller, T. Kaplan, and U. Landman, *Phys. Rev. B* **25**,

7255 (1982).

⁵R. Haydock and M. J. Kelly, *Surf. Sci.* **38**, 139 (1973).

⁶M. J. Kelly, in *Solid State Physics*, edited by H. Ehrenreich, F. Seitz, and D. Turnbull (Academic, New York, 1980), Vol. 35, p. 295.

⁷M. Mostoller and U. Landman, *Phys. Rev. B* **20**, 1755 (1979).

⁸See, for example, D. Castiel, L. Dobrzynski, and D. Spanjaard, *Surf. Sci.* **59**, 252 (1976).

⁹L. Dobrzynski and D. L. Mills, *J. Phys. Chem. Solids* **30**, 1043

- (1969).
- ¹⁰L. Dobrzynski and D. L. Mills, *Phys. Rev. B* **7**, 2367 (1973).
- ¹¹T. L. Einstein and J. R. Schrieffer, *Phys. Rev. B* **7**, 3629 (1973); T. L. Einstein, *ibid.* **12**, 1262 (1975).
- ¹²B. Laks and C. E. T. Gonçalves da Silva, *J. Phys. C* **10**, L99 (1977).
- ¹³R. E. DeWames and T. Wolfram, *Phys. Rev.* **185**, 720 (1969).
- ¹⁴D. L. Mills and A. A. Maradudin, *J. Phys. Chem. Solids* **28**, 1855 (1967).
- ¹⁵D. L. Mills, *J. Phys. (Paris) Colloq.* **31**, C1-33 (1970).
- ¹⁶H. I. Zhang, *Phys. Rev. B* **16**, 3194 (1977).
- ¹⁷G. Gumbs and A. Griffin, *Surf. Sci.* **91**, 669 (1980).
- ¹⁸F. Weling, *J. Phys. F* **10**, 1975 (1980).
- ¹⁹A. Yaniv, *Phys. Rev. B* **17**, 3904 (1978); **22**, 4776 (1980).
- ²⁰A. Yaniv, *Phys. Rev. B* **28**, 402 (1983).
- ²¹W. Ho, S. L. Cunningham, W. H. Weinberg, and L. Dobrzynski, *Phys. Rev. B* **12**, 3027 (1975); S. L. Cunningham, W. Ho, W. H. Weinberg, and L. Dobrzynski, *Appl. Surf. Sci.* **1**, 33 (1977); **1**, 44 (1977).
- ²²C. E. T. Gonçalves da Silva and B. Laks, *J. Phys. C* **10**, 851 (1977).
- ²³E.-Ni Foo, M. F. Thorpe, and D. Weaire, *Surf. Sci.* **57**, 323 (1976).
- ²⁴J. Tersoff and L. M. Falicov, *Phys. Rev. B* **24**, 754 (1981).
- ²⁵J. B. Salzberg and L. M. Falicov, *Phys. Rev. B* **15**, 5320 (1977).
- ²⁶W. Zinn, *J. Magn. Magn. Mater.* **3**, 23 (1976); also see H. A. Bohn, W. Zinn, B. Dorner, and A. Kollmar, *Phys. Rev. B* **22**, 5447 (1980).
- ²⁷See, for example, D. Castiel, *Surf. Sci.* **60**, 24 (1976).